HEMT-Based Read-out of a Thickness-Mode AlGaN/GaN Resonator

Azadeh Ansari and Mina Rais-Zadeh

Department of Electrical Engineering & Computer Science, University of Michigan, Ann Arbor, MI 48109, USA
Phone: (734)764-4249, Fax: (734)763-9324, Email: azadans@umich.edu

Abstract

A multi-gigahertz AlGaN/GaN resonator is introduced, where the fundamental thickness-mode resonance at 2.1 GHz is excited exhibiting a quality factor (Q) of 105. For the first time, acoustic strain in the vertical direction is excited and sensed through a two-dimensional electron gas (2DEG), induced at the AlGaN/GaN interface. The 2DEG sheet is used as the bottom electrode for piezoelectric actuation, as well as the transistor conduction channel for acoustic sensing. In this design, acoustic resonance is sensed by modulation of the HEMT drain current (I_D); thus, the transistor is biased in the linear region of operation. Here, we study the dependency of the acoustic transconductance on the readout HEMT biasing and show that the read-out HEMT senses the drain current modulation only when the 2DEG channel is not pinched. To use the full potential of the HEMT intrinsic amplification, the transistor needs to be biased in the saturation region, which would require a modified RB-HEMT design.

Introduction

AlGaN/GaN high electron mobility transistors have been widely used in broad-band power amplifiers in base station applications due to the high sheet carrier concentration, high electron mobility in the two-dimensional electron gas channel and high saturation velocity. The high electron sheet carrier concentration of nitride HEMTs is induced by piezoelectric and spontaneous polarization of the strained AlGaN layer. This suggests that III-nitride HEMT structures are very sensitive to mechanical pressure, which changes the piezoelectric polarization-induced surface and interface charges [1].
High-performance GaN micromechanical resonators have been reported previously with frequencies mostly lower than 1.5 GHz [2-4]. Extending the frequency of operation of passive piezoelectric MEMS resonators deeper into gigahertz regime is hindered due to issues associated with scaling of the device, such as larger capacitive feed-through levels. Furthermore, the amount of the piezoelectric charges that can be picked up is directly proportional to the area of the sensing electrodes and therefore the performance is limited when the device dimensions are scaled. Thus, an alternative read-out mechanism that could overcome the scaling issues is needed in order to push the resonant frequencies of GaN resonators to gigahertz regime where the GaN Integrated Circuits (ICs) generally operate at. Resonant body transistors (RBTs) can overcome such limitations and multi-GHz RBTs have been demonstrated in silicon [5].

While silicon-based RB transistors have been around for a number of years [5-7], the concept of RB HEMT is relatively new. An AlGaN/GaN Resonant HEMT was demonstrated in [8] and was used to excite the flexural-mode resonance of a beam with frequencies in lower megahertz range. In this work, we propose a four-terminal RB-HEMT that uses a back gate to launch acoustic wave into the vibrating body, exciting its thickness-mode resonance. The vertical acoustic strain propagates and is sensed through a read-out HEMT by detecting the change in its drain current (Fig. 1). We first proposed this structure in [4]; in this work, we explain the design principle and report the measurement results of fabricated devices in detail. Unlike [8], where flexural resonance modes are excited by a HEMT actuator placed at one end of a suspended beam and read out through a separate HEMT at the other end, the proposed device is more compact, has higher electromechanical coupling using the thickness-mode (e_{33}) piezoelectric coefficient, and can operate at higher frequencies.

The proposed RB-HEMT (Fig. 1) consists of four terminals: (1) a back gate Schottky contact (actuation top electrode), (2) a source ohmic contact used as the HEMT source terminal as well as the actuation bottom electrode, accessing the 2DEG channel, (3) a drain ohmic contact, located at the area of maximum displacement (sense output electrode), (4) a top gate Schottky contact (electrical signal tuning knob). The actuation principle is based on the piezoelectric properties of AlGaN layer sandwiched between the back gate Schottky contact and the bottom electrode (*i.e.* MIM structure). For efficient actuation, the AlGaN transduction layer has to be depleted of the induced charges and conduction must be limited to the AlGaN/GaN interface. The applied vertical electric field across the AlGaN layer induces a vertical mechanical strain in the hetero-structure that modulates the 2DEG mobility and carrier concentration, which is consequently reflected in the drain current (I_D). A fundamental thickness-mode resonance at 2.1 GHz is excited showing an acoustic transconductance of 15.5 µS with a Q of 105.
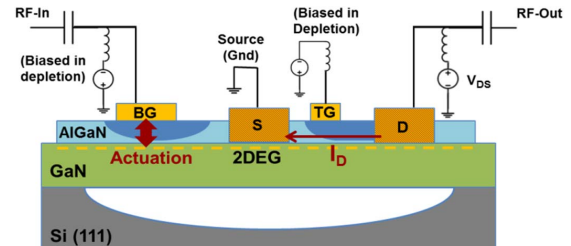

Fig. 1. RB-HEMT operation principle. The back gate is biased in depletion to avoid conduction through the AlGaN layer, and RF-signal is fed to the back gate Schottky contact (Port 1) for launching acoustic wave. 2DEG acts as the bottom electrode for acoustic excitation. Thickness-mode resonance is excited, inducing strain in the channel and modulating the drain current which is sensed through the drain contact (Port 2).

Fabrication

The RB-HEMTs are fabricated using Metal-Organic Chemical Vapor Deposition (MOCVD)-grown GaN-on-high-resistivity Si (111) as the starting wafer (Fig. 2(left)). Using GaN-on-Si, one can take advantage of the mature silicon technology for ease in releasing the structures as well as future hetero-integration with Si-CMOS. The total thickness of the GaN-based vibrating stack in this work is 1.8 μm, with a 175 Å thick AlGaN piezo active layer grown on top.

The fabrication starts with isolating the devices by removing the 2DEG outside of the mesa islands. Unlike [8] and [9], 2DEG is only interrupted outside of the resonator active area; thus, better Qs can be achieved because of the homogeneity in the mechanical structure. Ti/Al/Ti/Au is used for source and drain ohmic contact metallization followed by 30 seconds of annealing in nitrogen environment at 850 ˚C. Next, Ni/Au layer is deposited to form the back gate Schottky contact (for acoustic actuation) and the top gate Schottky contact (for electrical modulation of the 2DEG). Finally, vias were made through the GaN layer to access the Si layer, which is then isotropically etched by XeF$_2$. The cross-section of the starting wafer and the fabrication process flow are schematically shown in Fig. 2. A scanning electron microscope (SEM) image of the fabricated device is illustrated in Fig. 3.
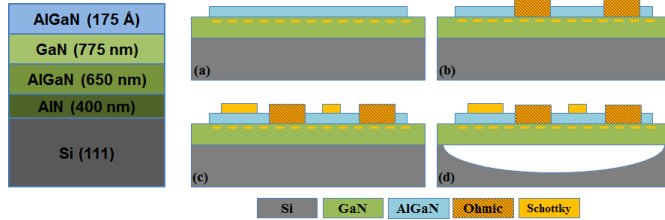

Fig. 2. (Left) Cross-section schematic of the GaN-on-Si starting wafer. The resonating stack consists of a total of ~1.8 μm thick AlN/ AlGaN/GaN layer and a 175 Å thick AlGaN transduction layer. (Right) Fabrication steps: (a) mesa isolation, (b) ohmic contact deposition and annealing, (c) Schottky contact formation, (d) Etching vias through GaN to access the Si layer and XeF$_2$ isotropic Si etching.
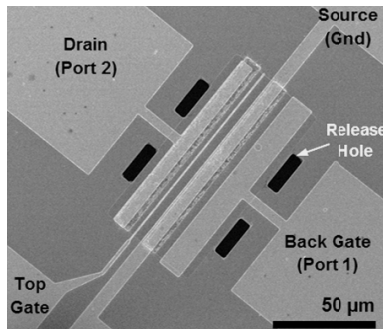

Fig. 3. SEM image of a fabricated RB-HEMT. Back gate, source, and drain contacts are each 6 μm ×100 μm. The top gate length is 1 um. Release holes were used for to access the Si substrate for XeF$_2$ isotropic etching.

Device Modeling

Equivalent circuit model of the RB-HEMT is shown in Fig. 4. The acoustic resonator is modeled with its Butterworth Van Dyke (BVD) equivalent circuit (R_m, C_m, and L_m). The mechanical branch is located between the back gate and source since alternating electric field is applied across the two of them. The parallel resistive (R_{2DEG}) and capacitive (C_p) branches model the parasitic electrical path. It must be noted that the 2DEG sheet is not interrupted between the back gate and the source in this design. The acoustic, g_a, back gate electrical, g_{mb}, and top gate electrical, g_m, transconductances are represented separately. g_a, g_{mb}, and g_m are all dependent on the top gate DC voltage, as will be discussed later. g_a is the acoustic transconductance, which has a small off-resonance value and peaks at the resonance frequency. g_{mb} represents the broad-band electrical back gate transconductance, appearing as a feed-through floor in the Y_{21}- Y_{12} plots.
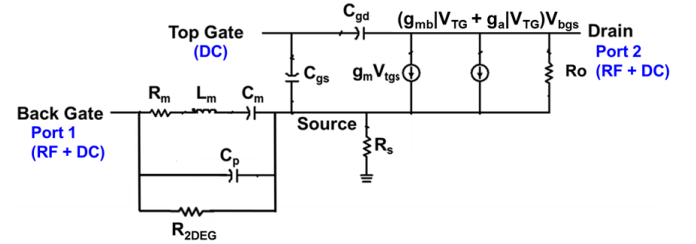

Fig. 4. Equivalent circuit model of the AlGaN/GaN RB-HEMT [10]. AC signal is fed to the back gate and collected from the drain. Acoustic actuation occurs between the back gate and the source contact. The induced acoustic wave modulates the drain current. g_{mb} models the back gate electric transconductance and g_a models the mechanical transconductance. Only DC voltage is applied to the top gate to keep the $g_m \times V_{tgs}$ contribution to the drain current small.

The drain current can be expressed as:

$$I_D = \mu_n \times \frac{W}{L} \times \rho_A \times V_{DS}, \qquad (1)$$

where W and L are the respective channel width and length, μ_n is electron mobility, and ρ_A is charge per unit area. The interface charge sheet density created under strain is:

$$\rho_A = [(\varepsilon_x + \varepsilon_y).(e_{31AlGaN} - e_{31GaN}) + \varepsilon_z.(e_{33AlGaN} - e_{33GaN})] \qquad (2)$$

$\varepsilon_x,, \varepsilon_y$, and ε_z are the strain tensors, and e_{31}, and e_{33} are the lateral and thickness-mode piezoelectric coefficients, respectively [8]. The drain current thus changes upon acoustic strain by:

$$\Delta I_D = \Delta(\mu_n \times \rho_A) \times \frac{W}{L} \times V_{DS}, \qquad (3)$$

The change in the 2DEG conductivity is in turn detected by sensing the drain current and is reflected in the total transconductance, from back gate to drain, as:

$$g_{mb} + g_a = \frac{\partial I_D}{\partial V_{BG}} = \frac{\partial(\mu_n \times \rho_A)}{\partial v_{bg(AC-in)}} \times \frac{W}{L} \times V_{DS}. \qquad (4)$$

Given the GaN-based stack with an AlGaN transduction layer of less than 20 nm, the electrode layout is optimized for efficient transduction. The vertical displacement of the RB-HEMT obtained using COMSOL 2D simulation tool [11] is provided in Fig. 5. The AlGaN/GaN interface is connected to the ground to model the 2DEG bottom electrode. The drain contact is placed at the location with maximum displacement,

and the source is located in the middle of the device at a nodal point with minimum displacement. Top gate only provides electrical signal tuning and is not included in the simulation.

It can be seen from the simulation that the maximum 2DEG conductivity modulation occurs under the drain region, explaining the reason for operating the read-out HEMT in the linear region of operation. As will be shown later, the output acoustic current shuts off when the channel gets pinched close to the drain area in the saturation region.
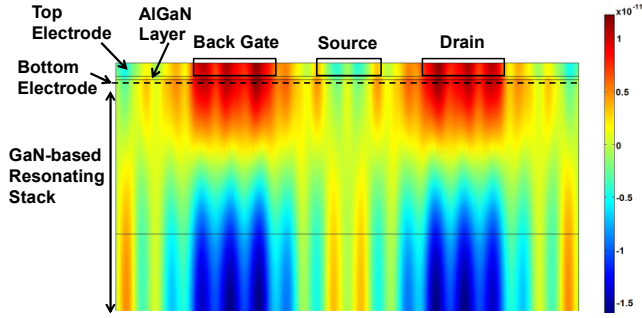

Fig. 5. 2D COMSOL simulation results showing the displacement along the thickness of the device at the fundamental thickness-mode resonance. The total GaN resonant stack thickness is 1.8 µm. The piezoelectric transduction layer is 175 Å thick AlGaN sandwiched between the top electrode and the 2DEG (modeled as the bottom electrode). The source contact, connected to ground, is placed in the middle of the RB-HEMT at a nodal point. Drain and back gate contacts are located at a location with maximum displacement.

Measurement Results and Discussion

RF measurements were carried out using a Lakeshore TTPX probe station, an Agilent N5241A PNA, and GSG ACP40 probes from Cascasde Microtech. Short-Open-Load-Through (SOLT) calibration was performed prior to all measurements. DC output characteristics of the read-out HEMTs were measured using a Keithly 4200-SCS parametric analyzer. All RF measurements were taken at room temperature and ambient pressure with 50 Ω termination impedances.

The actuation mechanism relies on the AlGaN layer depletion and limiting the conductance to the AlGaN/GaN interface charges. Actuators based on depletion forces have been shown [12], where the depletion width determines the capacitance value for electrostatic actuation. With the piezoelectric actuation however, the depletion width (in the thickness direction) determines the efficient thickness of the active piezoelectric layer sandwiched between the back gate (top electrode) and the 2DEG (bottom electrode). Thus, higher transduction occurs at larger negative potentials at the back gate, when the effective actuation layer thickness is maximum (Fig. 6). However, applying large negative signals to the back gate also results in pinching of the 2DEG (and removal of the bottom electrode) and thus the DC signal at the back gate should be smaller than the pinch-off threshold. Therefore, back gate is biased at V_{BG} = -1.8 V, for V_{AC}= 0.1 V, resulting in $\left| V_{BG} \right| + \left| V_{AC} \right| \leq \left| V_{BG\text{-pinch-off}} \right|$.

Fig. 6 shows the acoustic transconductance of the RB-HEMT, measured from the back gate to the drain. The feedthrough floor is de-embedded from the total Y_{21}- Y_{12} plot to

purely reflect the mechanical resonance. The static DC I-V characteristics of the read-out HEMT are shown in Fig. 7. The operation is maintained in the linear region to avoid channel pinching at the drain side.
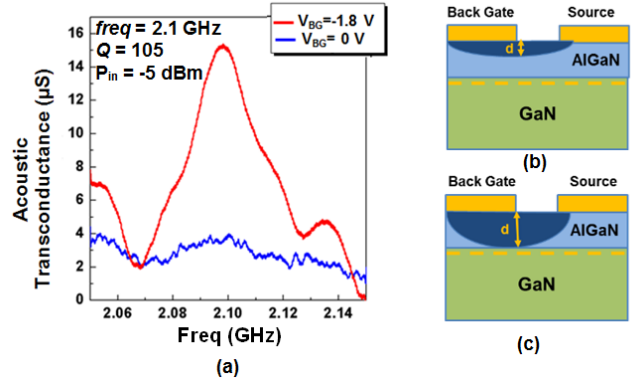

Fig. 6. (a) Acoustic transconductance of the AlGaN/GaN RB-HEMT. Maximum transconductance occurs at V_{BG}= -1.8 V, when V_{TG}= -1 V and V_{DS}= 0.1 V, and P_{in}=-5 dBm (V_{AC}=0.1 V). The acoustic transconductance amplitude reaches a maximum value of 15.5 µS at V_{BG}= -1.8 V. (b) Acoustic resonance does not get efficiently excited when the back gate is not in the reverse region of operation (*i.e.* V_{BG}= 0 V). (c) Maximum transduction occurs when the AlGaN layer under the back gate-source area is depleted but not pinched (*i.e.* V_{BG}+$V_{AC} \approx V_{BG\text{-pinch-off}}$= -1.9 V).
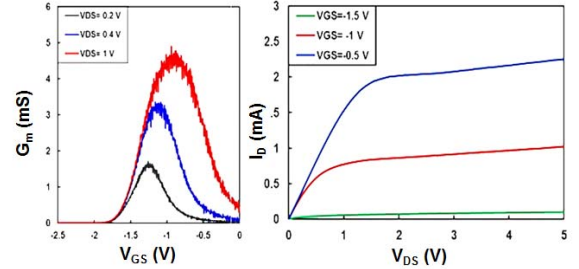

Fig. 7. Static DC characteristics of the read-out HEMT, consisting of the top gate, source, and drain contact (Back gate floating). (Left) Read-out HEMT transconductance (G_m) is plotted versus the top gate voltage (V_{TG}) at three different drain voltage DC bias voltages. It can be seen that the peak HEMT transconductance corresponds to higher top gate voltages as the drain voltage increases. (Right) I_D-V_{DS} curve of the transistor, showing a low knee voltage of ~$V_{DS\text{-SAT}}$= 0.5 V when biased at V_{GS}= -1 V.

The transconductance dependencies on top gate and drain DC voltages are investigated to prove that the read-out mechanism indeed relies on the modulation of 2DEG carrier density in the channel. Fig. 8 shows the total transconductance (Y_{21}-Y_{12}) at three different top gate voltages, when biased at V_{BG}= -1.8 V, and V_{DS}= 0.1 V. As shown, the RB-HEMT transconductance (g_a and g_{mb}) trends do not follow the read-out HEMT transconductance ($g_{m,}$ measured from the top gate to the drain). This is merely because of the design and physics of the RB-HEMT in this work. The externally applied AC voltage to the top gate is zero; when applying a larger negative DC signal to the top gate, the depletion region under the top gate-drain region grows and the acoustic transconductance decreases, whereas g_m increases. At V_{TG}= -1.5 V, the read-out HEMT channel gets pinched and the transistor turns off. Similarly, at a fixed

top gate DC voltage (Fig. 9), as the drain DC voltage increases, the depletion area between the top gate and the drain grows wider, until the channel gets pinched and no modulation occurs. V_{DSAT}= 0.5 V, marks the knee voltage when the read-out HEMT enters saturation region and consequently the acoustic output signal goes to zero.
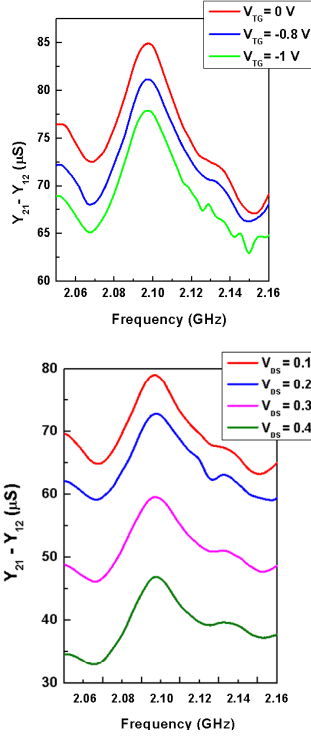

Fig. 8. RB-HEMT transconductance ($Y_{21} - Y_{12}$) dependency on the top gate voltage in the linear region (V_{BG}= -1.8 V, V_{DS}= 0.1 V). Transconductance is plotted at three different top gate voltages. The transconductance floor represents electrical modulation of the back gate voltage. At the resonance frequency (*freq*= 2.1 GHz), the transconductance curve rises about 16 μS higher than the feed-through

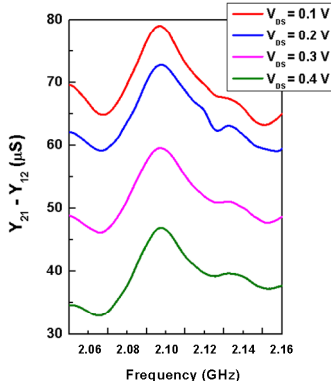**Fig. 9.** RB-HEMT $Y_{21} - Y_{12}$, transconductance, is plotted at four different drain-source voltages, when biased at V_{BG}= -1.8 V, and V_{TG}= -1 V with P_{in}= -5 dBm. The transconductance floor and peak value decreases with increasing the drain voltage. At V_{DS}= 0.5 V, which is the knee voltage when biased at V_{TG}= -1 V, the read-out HEMT can no longer sense the acoustic resonance as the 2DEG channel gets pinched at the area of maximum strain.

The feed-through floor seen in the transconductance plots is partly attributed to the back gate electrical transconductance (there is also a small $g_m \times V_{gs}$ contribution, which arises from the AC-voltage across the C_{GS}). The value of g_{mb} is measured as the slope of I_D versus the back gate voltage at low frequencies (Fig. 10). At V_{BG}= -1.8 V, the DC g_{mb} value (G_{mb}) is extracted to be ~30 μS.
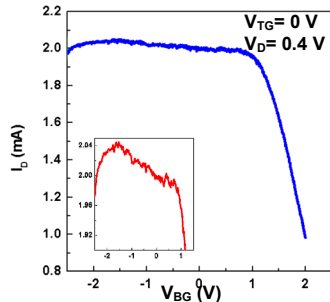

Fig. 10. DC I-V curve of the drain current versus the back gate voltage. The drain current is biased at I_D= 2 mA (V_{TG}= 0 V, and V_D = 0.4 V). V_{BG}= 0.7 V marks the turn-on voltage of the back gate Schottky diode. It must be noted that back gate Schottky contact is always kept in the reverse region of operation for efficient acoustic excitation (zoomed in the inset). The back gate electrical DC transconductance (G_{mb}) is derived from the slope of the I_D-V_{BG} plot at V_{BG}= -1.8 V.

Conclusion & Future Work

An AlGaN/GaN thickness-mode resonator was introduced, which uses HEMT-based sensing. The fundamental thickness-mode resonance is excited at *freq* = 2.1 GHz, showing a *Q* of 105. Higher order harmonics of the thickness-mode resonance can be effectively excited with smaller gate periphery. In this work, the sensing mechanism is based on the drain current modulation. The 2DEG mobility and carrier concentration gets locally modulated by the induced strain in the channel. The maximum strain is induced under the drain area of the channel, and thus channel pinching has to be avoided and the HEMT should be maintained in the linear region of operation. While current sensing is a solution for scaling the resonant frequency, in order to take advantage of the HEMT intrinsic amplification, the read-out HEMT has to operate in the saturation region, where induced piezoelectric charge at the top gate is boosted by the HEMT amplification and picked up at the drain. This is a subject of future work.

References

[1] S. J. Pearton, *et al.*, "GaN-based diodes and transistors for chemical, gas, biological and pressure sensing," *Journal of Phyics: Condensed Matter,* 16, R961–R994, 2004.

[2] V. J. Gokhale, J. Roberts, and M. Rais-Zadeh, "High-performance bulk-mode gallium nitride resonators and filters," *International Conference on Solid-State Sensors, Actuators and Microsystems*, pp. 926-929, Beijing, China, 2011.

[3] A. Ansari, *et al.*, "Gallium nitride-on-silicon micromechanical overtone resonators and filters," *IEEE Electron Device Meeting*, pp. 485-488, Washington, DC, 2011.

[4] A. Ansari, V. Gokhale, J. Roberts, and M. Rais-Zadeh, "Monolithic integration of GaN-based micromechanical resonators and HEMTs for timing application," *IEEE International Electron Device Meeting*, San Francisco, CA, 2012.

[5] D. Weinstein and S.A. Bhave, "The resonant body transistor," *Nano Letters*, Vol. 10, No. 4, pp. 1234-37, 2010.

[6] C. Durand, *et al.*, "In-plane silicon-on-nothing nanometer-scale resonant suspended gate MOSFET for in-IC integration perspectives,*" IEEE Electron Device Letters*, Vol. 29, No. 5, pp. 494-496, 2008.

[7] H. C. Nathanson, W. E. Newell, R.A. Wickstrom, and J. R. Davis, "The resonant gate transistor," *IEEE Trans. Electron Devices*, Vol. 14, No. 3, pp. 117-133, 1967.

[8] M. Faucher, *et al.*, "Electromechanical transductance of properties of a GaN MEMS resonator with fully integrated HEMT transducers," *Journal of Micromechanical Systems*, Vol. 21, No. 2, pp. 370-378, 2012.

[9] M. Faucher *et al.*, "Amplified piezoelectric transduction of nanoscale motion in gallium nitride electromechanical resonators," *Applied Physics Letters*, Vol. 94, Issue 23, pp. 233506, 2009.

[10] A. Ansari and M. Rais-Zadeh, "An AlGaN/GaN resonant body high electron mobility transistor," *IEEE Transaction on Electron Devices*, under review, 2013.

[11] COMSOL Home Page. http://www.comsol.com/ (accessed Sep. 16, 2013).

[12] J. H. Ransley, *et al.*, "Silicon depletion layer actuators," *Applied Physics Letters,* 92, 184103, 2008.